SCIENCE CHINA
Information Sciences

February 2021, Vol. 64 120303:1–120303:14
https://doi.org/10.1007/s11432-020-3090-5

• RESEARCH PAPER •
Special Focus on Ultra-Reliable Low-Latency Communications in Wireless Networks

Effective age of information in real-time wireless feedback control systems

Bo CHANG[1,2], Burak KIZILKAYA[1*], Liying LI[3], Guodong ZHAO[1], Zhi CHEN[2] & Muhammad Ali IMRAN[1]

[1]*School of Engineering, University of Glasgow, Glasgow* G12 8QQ, *UK;*
[2]*National Key Laboratory on Communications, University of Electronic Science and Technology of China* (*UESTC*), *Chengdu* 611731, *China;*
[3]*Department of Mathematics, Physics and Electrical Engineering, Northumbria University, Newcastle upon Tyne* NE1 8ST, *UK*

Received 28 May 2020/Revised 25 August 2020/Accepted 16 October 2020/Published online 20 January 2021

Abstract Ultra-reliable and low-latency communication (URLLC) is one of the most important scenarios in forthcoming fifth generation (5G) cellular networks to ensure timely exchange of information and realize real-time wireless control. In URLLC, timely information update needs to be guaranteed since control performance, e.g., control cost and stability, is directly determined by timely control information update. In this paper, we introduce an effective age of information (EAoI) to evaluate the timeliness of information update in control process. We consider the control process with two phases: sensor to controller phase and controller to actuator phase. We adopt first-generate-first-serve (FGFS) $M/M/1/1 \rightarrow M/M/1/2$ and FGFS $M/M/1/1^* \rightarrow M/M/1/2^*$ tandem queuing models to represent control process and we use finite-state Markov chains to describe control information updates. By studying state transitions, we calculate the average EAoI for both tandem queuing models. More importantly, we analyze throughput of wireless control systems and its relationship with average EAoI, which provides a guideline for URLLC system design in real-time feedback control systems. Simulation results show the advantage of using EAoI.

Keywords age of information, communications, feedback control, queuing, throughput, URLLC

Citation Chang B, Kizilkaya B, Li L Y, et al. Effective age of information in real-time wireless feedback control systems. Sci China Inf Sci, 2021, 64(2): 120303, https://doi.org/10.1007/s11432-020-3090-5

1 Introduction

The real-time wireless feedback control is a primary feature in many emerging application areas such as cyber-physical systems (CPS), industrial Internet of Things (IIoT), and Tactile Internet [1,2] where ultra-reliable and low-latency communication (URLLC) [3–7] is critical to ensure real-time control performance, e.g., control cost and stability. As shown in Figure 1, a typical real-time wireless feedback control system consists of two phases [8–13], i.e., Phase 1 from sensor to controller and Phase 2 from controller to actuator. To ensure system performance and stability, one of main requirements is the timely exchange of information between the two phases.

In Phase 1, the sensor measures the status of the plant and transmits updates to the controller via URLLC. This process is called status update and the timeliness of status update is measured by age of information (AoI) [14]. AoI is the amount of time elapsed since the moment that the freshest received update was generated. Current studies [15] on AoI generally consider status update, i.e., Phase 1. On the other hand, in Phase 2, the controller collects status updates and creates control commands accordingly. Then, it transmits control commands to the actuator to be executed. This process is called actuation update and timeliness of actuation update is studied in [16].

However, how to obtain AoI for the whole control process from sensors to actuators via controllers is still open and challenging. This is because the two phases in the control process are interdependent, where

* Corresponding author (email: b.kizilkaya.1@research.gla.ac.uk)

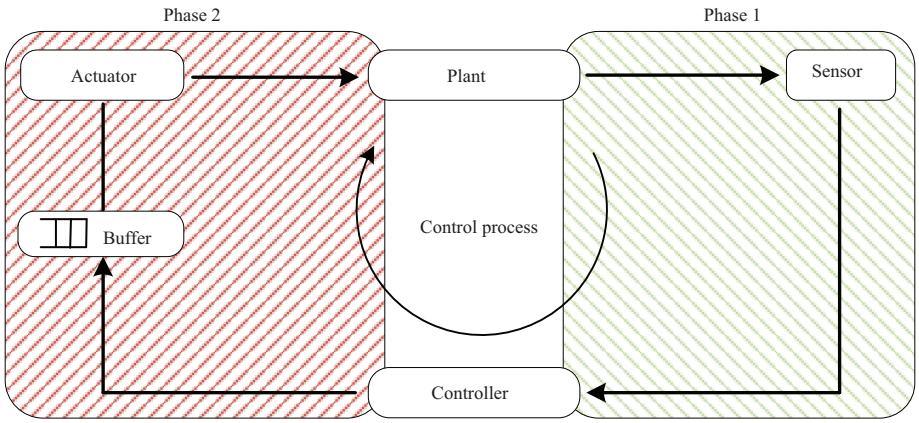

Figure 1 (Color online) A typical real-time wireless feedback control system with URLLC.

the failure of one phase will lead to invalidation of the other phase. Therefore, the whole control process should be treated as an end-to-end (E2E) link [10] rather than two independent links. Accordingly, in the calculation of AoI for the whole control process, we need to consider E2E links, rather than directly adding the AoIs of two phases.

In this paper, we define effective age of information (EAoI) which considers the whole control process from a sensor to an actuator as shown in Figure 1. The goal is to obtain the closed-form expression for the EAoI by tracking the whole control process. To achieve this goal, the key is to find suitable queuing models which represent the whole real-time feedback control process. Then, EAoI can be obtained by $\Delta(t) = t - L(t)$, where t represents the observation time at actuator and $L(t)$ represents the generated time of the latest sampled packet at sensor. Here, the main contributions of this paper are summarized as follows.

• We define EAoI, which is the time elapsed from the generation time of the last successful control process update until the time that current successful control process update is executed. This time duration is affected by sampling period, time delay, and packet loss which are critical parameters affecting control performance.

• We introduce two general first-generate-first-serve (FGFS) tandem queuing models according to the procedure of the control process. By studying state transition of the finite Markov chain for the adopted tandem queuing models, closed-form expressions of EAoI for real-time wireless feedback control system are obtained.

• We analyze throughput for the real-time wireless feedback control system based on average EAoI. Then, we discuss the relationship between EAoI-based throughput and parameters in the tandem queuing models, which gives a guideline for URLLC system design.

1.1 Related work

The AoI was firstly introduced in 1990s in real-time database systems to ensure the freshness of data [17, 18]. It is used as a metric to compare different synchronization techniques for databases. In recent years, a queuing theoretic approach was introduced in AoI research to analyze the age metric in various kinds of systems [15]. AoI became more important with the development of new technologies such as Internet of Things (IoT), smart cities, URLLC, and remote control systems.

Current researches on AoI usually considers source-to-destination links in sensor networks [14, 19–23]. For instance, the authors in [14] discussed the calculation of average AoI and peak AoI in direct source-to-destination link with different queuing models. In [19], the authors minimized AoI of status update for FGFS source-to-destination link by optimizing the arrival rate.

Moreover, there are other studies which consider AoI for source-to-destination link in specific scenarios [24–30]. For instance, the authors in [24] considered an energy harvesting source and optimized the AoI penalty in status update. In [26], the authors introduced the AoI into content update in a local cache, where they found that update rate in the cache is proportional to the square-root of items' popularity.

Furthermore, other studies have been done on wireless control systems [31–33]. For instance, the authors in [31] studied the usage of AoI in centralized scheduling problem for the real-time networked control with source-to-destination link. In [32], authors applied AoI to a wireless scheduling problem for

networked control systems. In [33], authors studied the impact of random AoI on the performance of cyber physical control systems. However, the above studies cannot be used to describe the whole control process in real-time wireless feedback control systems since sensor-to-controller and controller-to-actuator links are interdependent. In addition, these studies do not provide AoI definitions for real-time wireless feedback control systems. They use conventional AoI definition.

The studies that are most relevant to this paper are [34,35], where the authors analyzed the average AoI with a last-generate-first-serve (LGFS) tandem queuing model or multi-source queuing model in sensor networks since latest data is critical for sensor networks. However, the LGFS model cannot be used in real-time wireless feedback control systems since the control stability is determined by the ordinal data, which cannot be maintained by LGFS queuing model. On the contrary, the FGFS model is an exact match considering the process of real-time wireless feedback control. Furthermore, the AoI calculation methods in [34, 35] cannot be used for an FGFS model. This is because the packet discard strategies are significantly different between LGFS and FGFS models, where the previous packet should be discarded when the new packet comes for an LGFS model while it is exactly opposite for an FGFS model.

Considering existing literatures, the AoI definition for real-time wireless feedback control systems considering the whole control process from sensors to actuators via controllers is still an open and challenging problem. Accordingly, the calculation of AoI for the whole control process is missing. Therefore, we proposed the novel timeliness metric called EAoI for real-time wireless feedback control systems. We have also provided calculation of EAoI as well as analyzed throughput based on proposed new metric EAoI which provides foundation for further studies.

1.2 Organization

The rest of this paper is organized as follows. In Section 2, the system model and the EAoI definition are presented. In Section 3, the average EAoI is analyzed. In Section 4, the throughput for the real-time wireless feedback control systems is presented based on EAoI. In Section 5, simulation results are provided to demonstrate the performance. Finally, Section 6 concludes the paper.

2 System model and problem statement

As shown in Figure 1, we consider AoI and system throughput in a typical real-time wireless feedback control system [36, 37]. In such a system, the whole control process has two phases.

- Phase 1: the sensor takes samples of a plant, and sends them to the remote controller, where the corresponding control commands are calculated.
- Phase 2: the controller transmits control commands to the actuator. Then, the actuator executes the control commands, and updates the plant state.

Based on the above two phases, we introduce the definition of EAoI for each update in a control process.

Definition 1 (Effective age of information for control process)**.** For each update in a control process, the EAoI is defined by

$$\Delta(t_k) = t'_k - t_{k-1}, \tag{1}$$

where t'_k represents the time instant when the actuator finishes Phase 2 for the k-th control command, and t_{k-1} represents the time instant when a sensor starts Phase 1 for the $(k-1)$-th update.

Note that control performance, e.g., control cost or control stability, is closely related with EAoI, i.e., the time duration between t_{k-1} and t'_k. This time duration consists of sampling period of two contiguous successful control processes and time delay from sampling time instant to performing time instant of the corresponding control command at the actuator for each control process. This means that three critical parameters affecting control performance, i.e., sampling period, time delay, and packet loss [12], are indicated by EAoI. Thus, the proposed EAoI in this paper is critical for real-time wireless feedback control systems.

To calculate EAoI for each update in control process, we consider two typical tandem queuing models, i.e., FGFS $M/M/1/1 \to M/M/1/2$ tandem queuing model and $M/M/1/1^* \to M/M/1/2^*$ tandem queuing model, where the samples generated at the sensor follow the Poisson process with parameter λ, the update time for Phases 1 and 2 are exponentially distributed with update rate μ_1 and μ_2, respectively.

In FGFS $M/M/1/1 \rightarrow M/M/1/2$ tandem queuing model, for Phase 1, new arrival samples are discarded when the controller is busy; otherwise, they will be immediately transmitted and served by the controller. For Phase 2, a single control command packet will be kept when either condition in the following is satisfied:

- The actuator is idle;
- The actuator is busy, and the buffer is idle.

Otherwise, it will be discarded.

In FGFS $M/M/1/1^* \rightarrow M/M/1/2^*$ tandem queuing model, for Phase 1, a new sampled packet will be immediately transmitted and served by the controller. For Phase 2, a new control command packet will be served immediately when the actuator is idle, or will be kept in the buffer when the actuator is busy, or will replace the one that waits in the buffer when both the actuator and buffer are busy.

Based on the above system model and statements, we discuss the average EAoI calculation for control process update in Section 3.

3 Average effective age of information in real-time wireless feedback control systems

In this section, we first discuss the average EAoI for control process with an FGFS $M/M/1/1 \rightarrow M/M/1/2$ tandem queuing model in real-time wireless feedback control systems. Then, we analyze the average EAoI for control process with the FGFS $M/M/1/1^* \rightarrow M/M/1/2^*$ tandem queuing model.

3.1 Average EAoI for FGFS $M/M/1/1 \rightarrow M/M/1/2$

The states of FGFS $M/M/1/1 \rightarrow M/M/1/2$ tandem queuing model are $(0,0)$, $(1,0)$, $(0,1)$, $(1,1)$, $(0,2)$ and $(1,2)$, where the first and the second entries represent the states in Phases 1 and 2, respectively. For instance, the first entry indicates the state of Phase 1, i.e., 0 means Phase 1 is idle and 1 means it is busy. The second entry indicates the state of of Phase 2, i.e., 0 means that both actuator and buffer in Phase 2 are idle, 1 means the actuator is busy and the buffer is idle, and 2 means both actuator and buffer are busy.

The transition of the aforementioned states can be used in EAoI calculation, which can be described by a stochastic hybrid system (SHS) Markov chain as shown in Figure 2 [38]. For example, the state $(0,0)$ in Figure 2 will transfer to $(1,0)$ with rate λ when a new sampling packet is generated at the sensor. Other transitions in Figure 2 is similar with the above example when a new sample or a new control command is generated[1)].

Let S_i represent the system state when the i-th sampling packet arrives at the system, and $\pi_i(j) = \Pr(S_i = j)$ means that the system is under the state j when the i-th sampling packet arrives at the system. If the new generated sampling packet can be accessed in the system, the above six Markov states can be summarized by the following three states.

(1) "0": The controller in Phase 1 is idle, the actuator in Phase 2 is idle, and no control command is stored in the buffer. Then, "0" represents (0, 0) in Markov states.

(2) "1": The controller in Phase 1 is idle, the actuator in Phase 2 is busy, and no control command is stored in the buffer. Then, "1" represents (0, 1) in Markov states.

(3) "2": The controller in Phase 1 is idle, the actuator in Phase 2 is busy, and a control command is stored in the buffer. Then, "2" represents (0, 2) in Markov states.

To obtain the average EAoI for the n-th system update in a control process, the following two conditions should hold: (1) in Phase 1, the $(n-1)$-th sampling packet should complete service before the n-th sampling packet arriving; (2) in Phase 2, the $(n-1)$-th corresponding control command packet should leave the controller and is performed at the actuator before the n-th corresponding control command packet arriving at the actuator. Then, the probability that the first sample arrives at the system and finds that the system is under state "0" can be expressed as

$$\pi_1(0) = 1. \tag{2}$$

1) The self-transfer between states has no contributions to the calculation of effective AoI since the new arrival samples are discarded in Phase 1 when the controller is busy. Therefore, the self-transfer between states is not shown in an FGFS $M/M/1/1 \rightarrow M/M/1/2$ tandem queuing model.

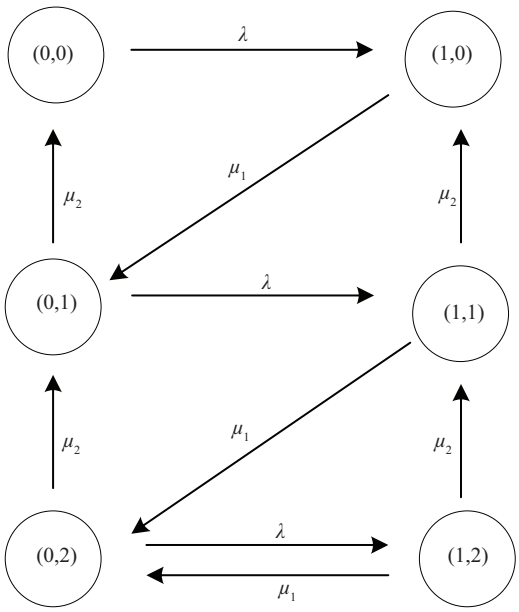

Figure 2 SHS Markov chain for $M/M/1/1 \to M/M/1/2$ tandem queue.

Then, the probability that the second sample arrives at the system and finds that the system is under state "0" can be expressed as

$$\pi_2(0) = \left(\frac{\mu_2}{\lambda+\mu_2}\right)\pi_1(0) = \frac{\mu_2}{\lambda+\mu_2}. \tag{3}$$

For $n \geqslant 3$, the probability that the new sample arrives at the system and finds that the system is under state "0" can be expressed as

$$\begin{aligned}\pi_n(0) &= \left(\frac{\mu_2}{\lambda+\mu_2}\right)\pi_{n-1}(0) + \left[\frac{\mu_2}{\lambda+\mu_2}\cdot\frac{\mu_2}{\mu_1+\mu_2} + \left(\frac{\mu_1}{\mu_1+\mu_2}\right)\cdot\left(\frac{\mu_2}{\lambda+\mu_2}\right)^2\right][1-\pi_{n-1}(0)] \\ &= \frac{\mu_2}{\lambda+\mu_2}\cdot\left[\left(1-\frac{\mu_1}{\mu_1+\mu_2}\cdot\frac{\lambda}{\lambda+\mu_2}\right) + \frac{\mu_1}{\mu_1+\mu_2}\cdot\frac{\lambda}{\lambda+\mu_2}\cdot\pi_{n-1}(0)\right] \\ &= \frac{\mu_2}{\lambda+\mu_2}\cdot\left(1-\frac{\mu_1}{\mu_1+\mu_2}\cdot\frac{\lambda}{\lambda+\mu_2}\right) + \frac{\mu_2}{\lambda+\mu_2}\cdot\frac{\mu_1}{\mu_1+\mu_2}\cdot\frac{\lambda}{\lambda+\mu_2}\cdot\pi_{n-1}(0). \end{aligned}\tag{4}$$

Based on (2)–(4), we can obtain the average EAoI for each system update. For the first update, the average effective EAoI can be expressed as

$$\Delta_{1,1} = \frac{1}{\lambda} + \frac{1}{\mu_1} + \frac{1}{\mu_2}. \tag{5}$$

For the n-th update, the average EAoI can be expressed as

$$\begin{aligned}\Delta_{1,n} &= \left(\frac{1}{\lambda}+\frac{1}{\mu_1}+\frac{1}{\mu_2}\right)\pi_n(0) + \left[\frac{\mu_2}{\mu_1+\mu_2}\left(\frac{1}{\mu_1}+\frac{1}{\mu_2}\right) + \frac{1}{\mu_2}\frac{\mu_1}{\mu_1+\mu_2}\right](1-\pi_n(0)) \\ &= \left(\frac{1}{\lambda}+\frac{1}{\mu_1}+\frac{1}{\mu_2}\right)\pi_n(0) + \left(\frac{1}{\mu_1}+\frac{1}{\mu_2}-\frac{1}{\mu_1+\mu_2}\right)(1-\pi_n(0)) \\ &= \frac{1}{\mu_1}+\frac{1}{\mu_2}-\frac{1}{\mu_1+\mu_2} + \left(\frac{1}{\lambda}+\frac{1}{\mu_1+\mu_2}\right)\pi_n(0), \end{aligned}\tag{6}$$

where $n \geqslant 2$.

3.2 Average EAoI for FGFS $M/M/1/1^* \to M/M/1/2^*$

The states of FGFS $M/M/1/1^* \to M/M/1/2^*$ tandem queuing model are $(0,0)$, $(1,0)$, $(0,1)$, $(1,1)$, $(0,2)$ and $(1,2)$, where the entries in each state have the same meaning as that in FGFS $M/M/1/1 \to$

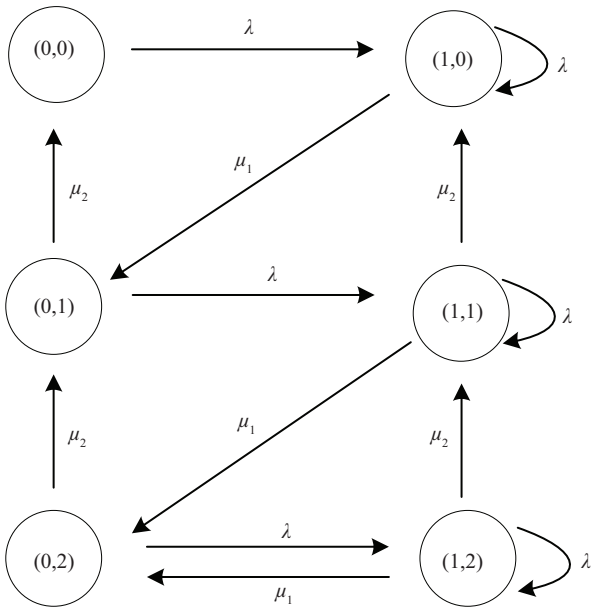

Figure 3 SHS Markov chain for $M/M/1/1^* \to M/M/1/2^*$ tandem queue.

$M/M/1/2$ tandem queuing model. The transition of the states can also be represented by SHS Markov chain, which is shown in Figure 3.

For FGFS $M/M/1/1^* \to M/M/1/2^*$ tandem queuing model, the access into the system is significantly different from that in FGFS $M/M/1/1 \to M/M/1/2$ tandem queuing model. In FGFS $M/M/1/1^* \to M/M/1/2^*$, samples are allowed to access when Phase 1 is either idle or busy. Furthermore, in Phase 2, the new generated control command can be transmitted to the actuator and served when the actuator is idle. On the other hand, the new generated control command should wait in the buffer when the actuator is busy. In summary, if the new generated sample can be accessed in Phase 1, the above six Markov states can be summarized by the following two states.

(1) "0": The controller in Phase 1 is idle/busy, and the actuator is idle in Phase 2. Then, "0" represents (0, 0) and (1, 0) in Markov states.

(2) "1": The controller in Phase 1 is idle/busy, and the actuator is busy in Phase 2. Then, "1" represents (0, 1), (0, 2), (1, 1) and (1, 2) in Markov states.

Then, the probability that the first sample arrives at the system and finds that the system is under state "0" can be expressed as

$$\pi_1'(0) = 1. \tag{7}$$

Then, the probability that the second sample arrives at the system and finds that the system is under state "0" can be expressed as

$$\pi_2'(0) = \frac{\mu_2}{\lambda + \mu_2}\pi_1'(0) = \frac{\mu_2}{\lambda + \mu_2}. \tag{8}$$

For $n \geqslant 3$, we have

$$\begin{aligned}\pi_n'(0) &= \left(\frac{\mu_2}{\lambda + \mu_2}\right)[\pi_{n-1}'(0) + \pi_{n-1}'(1)] \\ &= \left(\frac{\mu_2}{\lambda + \mu_2}\right)[\pi_{n-1}'(0) + (1 - \pi_{n-1}'(0))] \\ &= \frac{\mu_2}{\lambda + \mu_2}.\end{aligned} \tag{9}$$

Based on (7)–(9), we can obtain the average EAoI for each update in the control process. For the first update, the average EAoI can be expressed as

$$\Delta_{2,1} = \frac{1}{\lambda} + \frac{1}{\mu_1} + \frac{1}{\mu_2}. \tag{10}$$

For the n-th update, the average EAoI can be expressed as

$$\begin{aligned}\Delta_{2,n} &= \left(\frac{1}{\lambda}+\frac{1}{\mu_1}+\frac{1}{\mu_2}\right)\pi'_n(0)+\left[\frac{\mu_2}{\mu_1+\mu_2}\left(\frac{1}{\mu_1}+\frac{1}{\mu_2}\right)+\frac{1}{\mu_2}\frac{\mu_1}{\mu_1+\mu_2}\right](1-\pi'_n(0))\\ &= \left(\frac{1}{\lambda}+\frac{1}{\mu_1}+\frac{1}{\mu_2}\right)\pi'_n(0)+\left(\frac{1}{\mu_1}+\frac{1}{\mu_2}-\frac{1}{\mu_1+\mu_2}\right)(1-\pi'_n(0))\\ &= \frac{1}{\mu_1}+\frac{1}{\mu_2}-\frac{1}{\mu_1+\mu_2}+\left(\frac{1}{\lambda}+\frac{1}{\mu_1+\mu_2}\right)\pi'_n(0),\end{aligned} \tag{11}$$

where $n \geqslant 2$.

4 Throughput for real-time wireless feedback control systems

In this section, we investigate the system throughput based on the average EAoI for each system update in control process. Specifically, we first analyze system throughput in FGFS $M/M/1/1 \to M/M/1/2$ based on the average EAoI $\Delta_{1,n}$. Then, we study system throughput in FGFS $M/M/1/1^* \to M/M/1/2^*$ based on the average EAoI $\Delta_{2,n}$.

4.1 Throughput for FGFS $M/M/1/1 \to M/M/1/2$

4.1.1 *Average EAoI based throughput*

Based on the average EAoI for each system update n in FGFS $M/M/1/1 \to M/M/1/2$, we can obtain the average total time $D_{1,n}$ elapsing in the system. When n is equal to 1, i.e., $n = 1$, we can obtain $D_{1,1}$ as

$$D_{1,1} = \Delta_{1,1} = \frac{1}{\lambda}+\frac{1}{\mu_1}+\frac{1}{\mu_2}. \tag{12}$$

Then, for $n \geqslant 2$, we have

$$\begin{aligned}D_{1,n} &= D_{1,n-1}+\Delta_{1,n}\\ &= D_{1,n-2}+\Delta_{1,n-1}+\Delta_{1,n}\\ &= D_{1,1}+\Delta_{1,2}+\cdots+\Delta_{1,n}\\ &= \Delta_{1,1}+\Delta_{1,2}+\cdots+\Delta_{1,n}.\end{aligned} \tag{13}$$

Substituting (5) and (6) into (13), $D_{1,n}$ can be obtained as

$$\begin{aligned}D_{1,n} &= \Delta_{1,1}+\Delta_{1,2}+\cdots+\Delta_{1,n}\\ &= n\cdot A+B\left(\sum_{i=1}^{n}\pi_n(0)\right),\end{aligned} \tag{14}$$

where

$$A = \frac{1}{\mu_1}+\frac{1}{\mu_2}-\frac{1}{\mu_1+\mu_2}, \tag{15}$$

and

$$B = \frac{1}{\lambda}+\frac{1}{\mu_1+\mu_2}. \tag{16}$$

Then, the system throughput can be obtained as

$$\rho_1 = \lim_{n\to\infty}\frac{n}{D_{1,n}} = \lim_{n\to\infty}\frac{n}{n\cdot A+B\left(\sum_{i=1}^{n}\pi_n(0)\right)}. \tag{17}$$

In (17), we have

$$\sum_{i=1}^{n}\pi_n(0) = \pi_1(0)\frac{1-b^n}{1-b}-\frac{a}{1-b}\left(\frac{1-b^n}{1-b}-n\right)$$

$$= \frac{1-b^n}{1-b} - \frac{a}{1-b}\left(\frac{1-b^n}{1-b} - n\right), \tag{18}$$

where

$$a = \frac{\mu_2}{\lambda+\mu_2} \cdot \left(1 - \frac{\mu_1}{\mu_1+\mu_2} \cdot \frac{\lambda}{\lambda+\mu_2}\right), \tag{19}$$

and

$$b = \frac{\mu_2}{\lambda+\mu_2} \cdot \frac{\mu_1}{\mu_1+\mu_2} \cdot \frac{\lambda}{\lambda+\mu_2}. \tag{20}$$

Then, the system throughput in (17) can be further written as

$$\begin{aligned}\rho_1 &= \lim_{n\to\infty} \frac{n}{D_{1,n}} \\ &= \lim_{n\to\infty} \frac{n}{n \cdot A + B(\frac{1-b^n}{1-b} - \frac{a}{1-b}(\frac{1-b^n}{1-b} - n))} \\ &= \frac{1}{A + B \cdot \frac{a}{1-b}}.\end{aligned} \tag{21}$$

From the above discussion, the system throughput is determined by the accumulation of the average EAoI for each system update in the control process. Next, we analyze the relationship between the throughput and the update rate μ_1 in Phase 1 and μ_2 in Phase 2.

4.1.2 *Relationship between throughput and update rate in EAoI*

We assume the throughput is represented by $\rho_{1,1}$ when the update rate μ_1 for Phase 1 is greater than the update rate μ_2 for Phase 2, i.e., $\mu_1 > \mu_2$. On the contrary, the throughput is represented by $\rho_{1,2}$ when the update rate μ_1 for Phase 1 is less than or equal to the update rate μ_2 for Phase 2, i.e., $\mu_1 \leqslant \mu_2$. Then, from (21), we have

$$\begin{aligned}\frac{1}{\rho_{1,1}} - \frac{1}{\rho_{1,2}} &= (A_1 - A_2) + \left(B_1\frac{a_1}{1-b_1} - B_2\frac{a_2}{1-b_2}\right) \\ &= B_1\left(\frac{a_1}{1-b_1} - \frac{a_2}{1-b_2}\right),\end{aligned} \tag{22}$$

where $A_1 = A_2 = \frac{1}{\mu_1} + \frac{1}{\mu_2} - \frac{1}{\mu_1+\mu_2}$, $B_1 = B_2 = \frac{1}{\lambda} + \frac{1}{\mu_1+\mu_2}$, $a_1 = \frac{\mu_2}{\lambda+\mu_2} \cdot (1 - \frac{\mu_1}{\mu_1+\mu_2} \cdot \frac{\lambda}{\lambda+\mu_2})$, $a_2 = \frac{\mu_1}{\lambda+\mu_1} \cdot (1 - \frac{\mu_2}{\mu_1+\mu_2} \cdot \frac{\lambda}{\lambda+\mu_1})$, $b_1 = \frac{\mu_2}{\lambda+\mu_2} \cdot \frac{\mu_1}{\mu_1+\mu_2} \cdot \frac{\lambda}{\lambda+\mu_2}$, and $b_2 = \frac{\mu_1}{\lambda+\mu_1} \cdot \frac{\mu_2}{\mu_1+\mu_2} \cdot \frac{\lambda}{\lambda+\mu_1}$.
In (22), we have

$$\begin{aligned}\frac{1-b_1}{a_1} - \frac{1-b_2}{a_2} &= \left(1 - \frac{\mu_2}{\lambda+\mu_2} \cdot \frac{\mu_1}{\mu_1+\mu_2} \cdot \frac{\lambda}{\lambda+\mu_2}\right)\frac{\lambda+\mu_2}{\mu_2} - \left(1 - \frac{\mu_1}{\lambda+\mu_2} \cdot \frac{\mu_2}{\mu_1+\mu_2} \cdot \frac{\lambda}{\lambda+\mu_1}\right)\frac{\lambda+\mu_1}{\mu_1} \\ &= \frac{\lambda(\mu_1-\mu_2)}{\mu_1\mu_2} + \frac{\lambda}{\mu_1+\mu_2}\left(\frac{\mu_2}{\lambda+\mu_1} - \frac{\mu_1}{\lambda+\mu_2}\right) \\ &= \frac{\lambda^2(\mu_1^2-\mu_2^2) + \lambda(\mu_1^3-\mu_2^3) + 2\lambda\mu_1\mu_2(\mu_1-\mu_2) + 2\mu_1\mu_2(\mu_1^2-\mu_2^2)}{\mu_1\mu_2(\mu_1+\mu_2)(\lambda+\mu_1)(\lambda+\mu_2)}.\end{aligned} \tag{23}$$

Then, we can obtain $\frac{1-b_1}{a_1} - \frac{1-b_2}{a_2} > 0$ and $\frac{1}{\rho_{1,1}} - \frac{1}{\rho_{1,2}} < 0$ in (22), which means that $\rho_{1,1} > \rho_{1,2}$. According to the update rates for Phases 1 and 2, we have the following two cases.

(1) Case I: update rate μ_1 for Phase 1 is greater than update rate μ_2 for Phase 2, i.e., $\mu_1 > \mu_2$.

(2) Case II: update rate μ_1 for Phase 1 is less than or equal to update rate μ_2 for Phase 2, i.e., $\mu_1 \leqslant \mu_2$.

Then, the following property can be obtained.

Property 1. In real-time wireless feedback control systems with $M/M/1/1 \to M/M/1/2$ tandem queuing model, the average system throughput for Case I is greater than that for Case II. Furthermore, since average throughput is accumulated by inverse of the average EAoI for each system update in the control process, the average EAoI for Case I is less than that for Case II.

4.2 Throughput for FGFS $M/M/1/1^* \to M/M/1/2^*$

4.2.1 *Average EAoI based throughput*

Based on the average EAoI for each system update n in FGFS $M/M/1/1^* \to M/M/1/2^*$, we can obtain the average total time $D_{2,n}$ elapsing from the system. For the first update, i.e., $n = 1$, we can obtain $D_{2,1}$ as

$$D_{2,1} = \Delta_{2,1} = \frac{1}{\lambda} + \frac{1}{\mu_1} + \frac{1}{\mu_2}. \tag{24}$$

Then, for $n \geqslant 2$, we have

$$D_{2,n} = \Delta_{2,1} + \Delta_{1,2} + \cdots + \Delta_{2,n}. \tag{25}$$

Substituting (10) and (11) into (25), we can obtain $D_{2,n}$ as

$$D_{2,n} = n \cdot A + B\left(\sum_{i=1}^{n} \pi'_n(0)\right), \tag{26}$$

where A and B are obtained in (15) and (16), respectively. Then, the system throughput can be obtained as

$$\rho_2 = \lim_{n\to\infty} \frac{n}{D_{2,n}} = \lim_{n\to\infty} \frac{n}{n \cdot A + B\left(\sum_{i=1}^{n} \pi'_n(0)\right)}. \tag{27}$$

In (27), we have

$$\sum_{i=1}^{n} \pi'_n(0) = \frac{\lambda + n\mu_2}{\lambda + \mu_2}. \tag{28}$$

Then, the system throughput in (27) can be further written as

$$\begin{aligned} \rho_2 &= \lim_{n\to\infty} \frac{n}{n \cdot A + B(\frac{\lambda+n\mu_2}{\lambda+\mu_2})} \\ &= \frac{1}{A + B \cdot \frac{\mu_2}{\lambda+\mu_2}}. \end{aligned} \tag{29}$$

Similar with FGFS $M/M/1/1 \to M/M/1/2$, the system throughput in FGFS $M/M/1/1^* \to M/M/1/2^*$ is also determined by the accumulation of EAoI. Next, we analyze the relationship between the throughput and update rates μ_1 and μ_2.

4.2.2 *Relationship between throughput and update rate in EAoI*

We assume the throughput is represented by $\rho_{2,1}$ when the update rate μ'_1 for Phase 1 is greater than the update rate μ'_2 for Phase 2, i.e., $\mu'_1 > \mu'_2$. On the contrary, the throughput is represented by $\rho_{2,2}$ when the update rate μ'_1 for Phase 1 is less than or equal to the update rate μ'_2 for Phase 2, i.e., $\mu'_1 \leqslant \mu'_2$. Then, from (29), we have

$$\frac{1}{\rho_{2,1}} - \frac{1}{\rho_{2,2}} = B'_1\left(\frac{\mu'_2}{\lambda + \mu'_2} - \frac{\mu'_1}{\lambda + \mu'_1}\right), \tag{30}$$

where $B'_1 = \frac{1}{\lambda} + \frac{1}{\mu'_1+\mu'_2}$. In (30), we have

$$\frac{\mu'_2}{\lambda + \mu'_2} - \frac{\mu'_1}{\lambda + \mu'_1} < 0. \tag{31}$$

When $\mu'_1 > \mu'_2$, we can obtain $\frac{1}{\rho_{2,1}} - \frac{1}{\rho_{2,2}} < 0$ in (30), which means that $\rho_{2,1} > \rho_{2,2}$. Based on the above discussion, the following property can be obtained for FGFS $M/M/1/1^* \to M/M/1/2^*$, which is the same with $M/M/1/1 \to M/M/1/2$ tandem queuing model in Property 1.

Property 2. In real-time wireless feedback control systems with $M/M/1/1^* \to M/M/1/2^*$ tandem queuing model, the average system throughput for Case I is greater than that for Case II. Furthermore, since average throughput is accumulated by inverse of the average EAoI, the average EAoI for Case I is less than that for Case II.

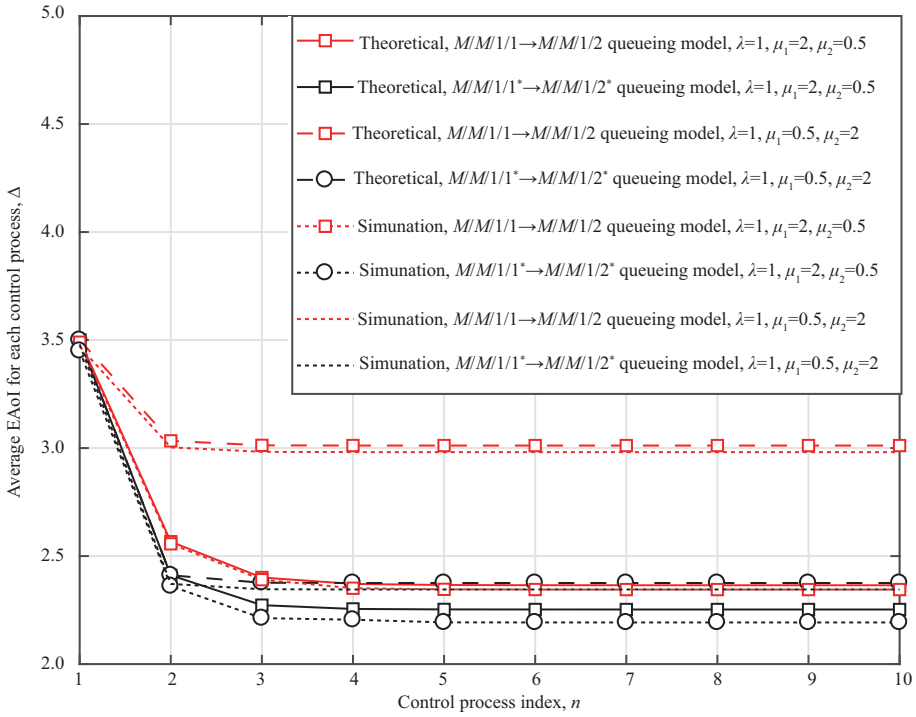

Figure 4 (Color online) Average EAoI for each system update n in the control process with different tandem queuing models.

5 Numerical results

In this section, we provide numerical results to demonstrate the average EAoI and its relationship with the overall system throughput in real-time wireless feedback control systems. For the adopted FGFS $M/M/1/1 \to M/M/1/2$ tandem queuing model and FGFS $M/M/1/1^* \to M/M/1/2^*$ tandem queuing model, we assume that the arrival rate of Poisson process for samples is $\lambda = 1$. Furthermore, the update rates μ_1 and μ_2 are variables according to different performance simulations.

Figure 4 shows the performance of average EAoI for each system update n in control process with different tandem queuing models given different update rates μ_1 and μ_2. From the figure, all four curves with different μ_1 and μ_2 first decrease and then maintain horizontal with n increasing for both $M/M/1/1 \to M/M/1/2$ tandem queuing model and $M/M/1/1^* \to M/M/1/2^*$ tandem queuing model. The average EAoI in either (6) for $M/M/1/1 \to M/M/1/2$ or (11) for $M/M/1/1^* \to M/M/1/2^*$ changes with the probability $\pi_n(0)$ or $\pi'_n(0)$ linearly. At the first three system updates, i.e., $n \leqslant 3$, both $\pi_n(0)$ and $\pi'_n(0)$ will decrease. Then, the system is stable when $n > 3$, where both $\pi_n(0)$ and $\pi'_n(0)$ will be constant. Thus, the changes of the four curves with system update n are reasonable. Furthermore, considering $n > 3$, e.g., $n = 5$, the average EAoI of the case when $\mu_1 > \mu_2$ is smaller than that when $\mu_1 < \mu_2$ for the both two adopted tandem queuing models. The reason can be obtained by comparing (6) (or (11)) with different assumptions $\mu_1 > \mu_2$ and $\mu_1 < \mu_2$, which are also corresponding with Properties 1 and 2, i.e., the average EAoI when $\mu_1 > \mu_2$ is less than that when $\mu_1 < \mu_2$. In addition, comparing the curves with the same μ_1 and μ_2 for $M/M/1/1 \to M/M/1/2$ tandem queuing model and $M/M/1/1^* \to M/M/1/2^*$ tandem queuing model, e.g., $\mu_1 = 2$ and $\mu_2 = 0.5$, the curve of $M/M/1/1^* \to M/M/1/2^*$ tandem queuing model is below that of $M/M/1/1 \to M/M/1/2$ tandem queuing model, which indicates that $M/M/1/1^* \to M/M/1/2^*$ tandem queuing model outperforms $M/M/1/1 \to M/M/1/2$ tandem queuing model in terms of EAoI. Furthermore, the comparison of the theory results and numerical results is shown in Figure 4, where the performance loss is minor and can be ignored. In the following of this section, we use the theoretical results to show the performance of the proposed method.

Figure 5 illustrates the performance of the average EAoI for system update $n = 5$ in different tandem queuing models with different update rate μ_1 and μ_2, where average EAoIs Δ_1 and Δ_2 are shown in Figures 5(a) and (b) for $M/M/1/1 \to M/M/1/2$ tandem queuing model and $M/M/1/1^* \to M/M/1/2^*$ tandem queuing model, respectively. From the figure, the average EAoIs strictly decrease with increasing μ_1 and μ_2. Furthermore, when μ_1 and μ_2 are large enough, the average EAoIs Δ_1 and Δ_2 will be stable

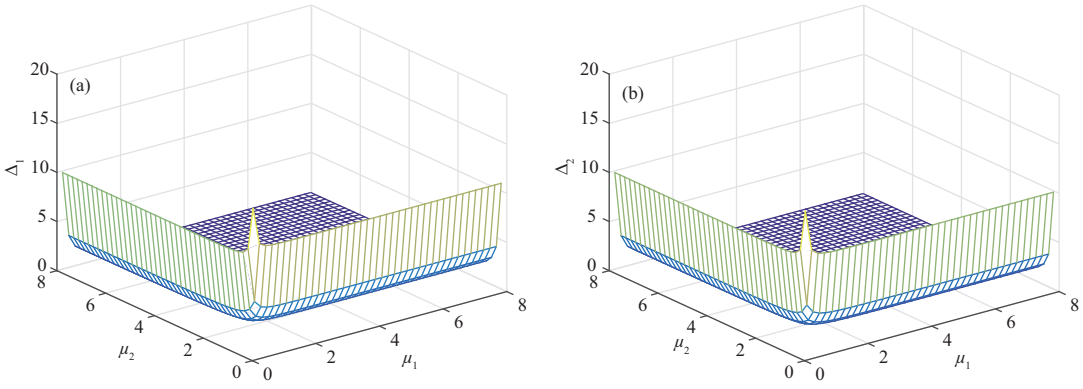

Figure 5 (Color online) Average EAoI for system update $n = 5$ in different tandem queuing models with different update rate μ_1 and μ_2. (a) $M/M/1/1 \to M/M/1/2$ tandem queuing model; (b) $M/M/1/1^* \to M/M/1/2^*$ tandem queuing model.

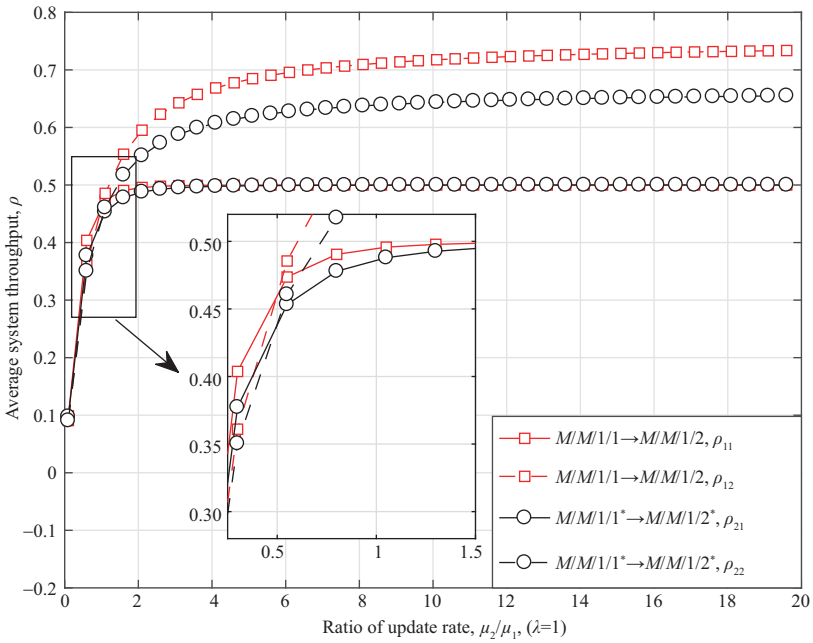

Figure 6 (Color online) Average throughput with different ratio μ_2/μ_1 for different queuing models.

with little changes. This is reasonable because both Eqs. (6) and (11) will be constant when $\mu_1 \to \infty$ and $\mu_2 \to \infty$.

Figure 6 shows the performance of average throughput with different ratios of update rates μ_2/μ_1 for different tandem queuing models, where we have $\lambda = 1$. From the figure, all throughput curves first increase with respect to μ_2/μ_1 ratio, then reach a saturate value when the ratio is large enough for both $M/M/1/1 \to M/M/1/2$ tandem queuing model and $M/M/1/1^* \to M/M/1/2^*$ tandem queuing model. This is reasonable because both Eqs. (21) and (29) will be constant when μ_1 and μ_2 are large enough. In addition, when $\mu_2 < \mu_1$, i.e., $\mu_2/\mu_1 < 1$, the throughput of Case I (i.e., the rate of Phase 1 is higher than the rate of Phase 2) is higher than that of Case II (i.e., the rate of Phase 1 is smaller than the rate of Phase 2) for the two queuing models. The reason can be obtained by Properties 1 and 2. On the other hand, when $\mu_2 > \mu_1$, i.e., $\mu_2/\mu_1 > 1$, the throughput of Case I is smaller than that of Case II. When the throughput is stable and saturate, we can obtain that the performance gains of Case II are about 50% and 35% compared with Case I for $M/M/1/1 \to M/M/1/2$ and $M/M/1/1^* \to M/M/1/2^*$ tandem queuing models, respectively.

Furthermore, in Figure 6, given λ, μ_1, and μ_2, the throughput of the $M/M/1/1^* \to M/M/1/2^*$ tandem queuing model is smaller than that of the $M/M/1/1 \to M/M/1/2$ tandem queuing model, because the throughput is the inverse of the accumulation of the EAoI. Therefore, the relationship of throughput is in contrast to the EAoI for the two models.

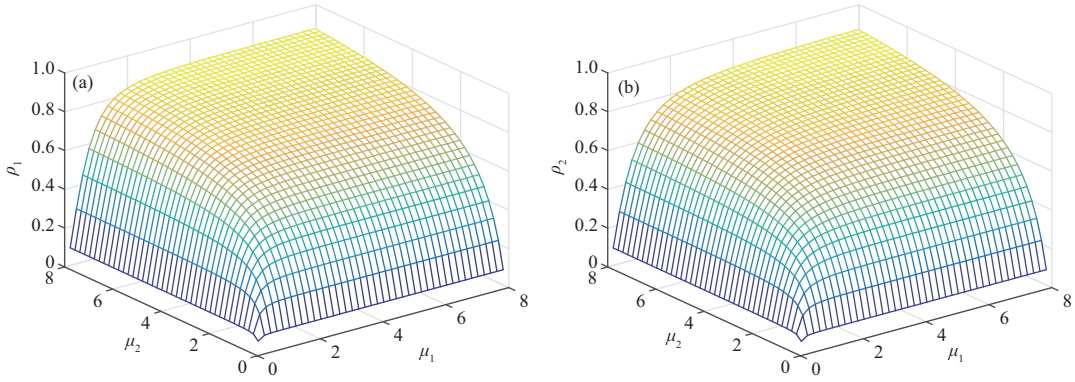

Figure 7 (Color online) Average throughput for different tandem queuing models with different process rates μ_1 and μ_2. (a) $M/M/1/1 \to M/M/1/2$ tandem queuing model. (b) $M/M/1/1^* \to M/M/1/2^*$ tandem queuing model.

Figure 7 illustrates the performance of average throughput for different tandem queuing models with different process rate μ_1 and μ_2, where average throughputs ρ_1 and ρ_2 are shown in Figures 7(a) and (b) for $M/M/1/1 \to M/M/1/2$ tandem queuing model and $M/M/1/1^* \to M/M/1/2^*$ tandem queuing model, respectively. From the figure, the average throughputs in both Figures 7(a) and (b) increase with μ_1 and μ_2. Furthermore, when μ_1 and μ_2 are large enough, the average throughput ρ_1 and ρ_2 will be stable with minor changes, where the reason is the same as that in Figure 5.

6 Conclusion

In this paper, EAoI is proposed for real-time wireless control systems which is a critical metric because it indicates both latency and packet loss in URLLC. To describe the whole process from sensors to actuators, we adopted two FGFS tandem queuing models, i.e., FGFS $M/M/1/1 \to M/M/1/2$ tandem queuing model and FGFS $M/M/1/1^* \to M/M/1/2^*$ tandem queuing model, where the difference between them is that the new arrival packet will replace the existing packet in FGFS $M/M/1/1^* \to M/M/1/2^*$ tandem queuing model. Then, the stochastic hybrid system Markov chain was introduced to analyze the two tandem queuing models. Based on that, we calculated EAoI for each system update. More importantly, we analyzed the relationship between system throughput and EAoI. This provides a guideline for URLLC system design in real-time feedback control systems. (1) Both update rates μ_1 in Phase 1 and μ_2 in Phase 2 should be large to reduce EAoI; (2) μ_2 should be larger than μ_1 to increase the system throughput; (3) there is minor effect on EAoI and throughput when μ_1 and μ_2 are larger than a certain threshold. As a future work, optimization of update rates will be studied using proposed EAoI metric to achieve certain level of performance in real-time wireless feedback control systems. In addition, the tail behaviour of the AoI may also be useful to represent extreme situations in some scenarios. However, it is extremely challenging to analyze the tail behaviour in tandem queueing model. Therefore, addressing this issue would be our future work. Design aspects of the proposed metric are also crucial for system design and system performance. One of the main design difficulties could be the time synchronization of the two phases of the control process to effectively use the proposed EAoI metric, because the first phase and the second phase of the control process take place in different physical locations.

Acknowledgements This work was supported in part by National Natural Science Foundation of China (Grant No. 61631004).

References

1 Lu C, Saifullah A, Li B, et al. Real-time wireless sensor-actuator networks for industrial cyber-physical systems. Proc IEEE, 2016, 104: 1013–1024

2 Sato K, Kawamoto Y, Nishiyama H, et al. A modeling technique utilizing feedback control theory for performance evaluation of IoT system in real-time. In: Proceedings of International Conference on Wireless Communications & Signal Processing (WCSP), 2015. 1–5

3 Hößler T, Simsek M, Fettweis G P. Mission reliability for URLLC in wireless networks. IEEE Commun Lett, 2018, 22: 2350–2353

4 Singh B, Tirkkonen O, Li Z, et al. Contention-based access for ultra-reliable low latency uplink transmissions. IEEE Wirel Commun Lett, 2018, 7: 182–185

5 Nielsen J J, Liu R, Popovski P. Ultra-reliable low latency communication using interface diversity. IEEE Trans Commun, 2018, 66: 1322–1334

6 She C, Yang C, Quek T Q S. Radio resource management for ultra-reliable and low-latency communications. IEEE Commun Mag, 2017, 55: 72–78

7 She C, Yang C, Quek T Q S. Cross-layer optimization for ultra-reliable and low-latency radio access networks. IEEE Trans Wireless Commun, 2018, 17: 127–141

8 Geng H, Alto P. Internet of Things and Data Analytics Handbook. Piscataway: Wiley Press, 2016

9 3GPP. Study on Communication for Automation in Vertical Domains. TR 22804. 2018. https://www.tech-invite.com/3m22/tinv-3gpp-22-804.html

10 Chang B, Zhang L, Li L, et al. Optimizing resource allocation in URLLC for real-time wireless control systems. IEEE Trans Veh Technol, 2019, 68: 8916–8927

11 Chang B, Zhao G, Chen Z, et al. Packet-drop design in URLLC for real-time wireless control systems. IEEE Access, 2019, 7: 183081

12 Chang B, Zhao G, Zhang L, et al. Dynamic communication QoS design for real-time wireless control systems. IEEE Sens J, 2020, 20: 3005–3015

13 Chang B, Zhao G, Chen Z, et al. D2D transmission scheme in URLLC enabled real-time wireless control systems for tactile internet. In: Proceedings of IEEE Global Communications Conference, 2019. 1–6

14 Costa M, Codreanu M, Ephremides A. On the age of information in status update systems with packet management. IEEE Trans Inform Theor, 2016, 62: 1897–1910

15 Kaul S, Gruteser M, Rai V, et al. Minimizing age of information in vehicular networks. In: Proceedings of the 8th Annual IEEE Communications Society Conference on Sensor, Mesh and Ad Hoc Communications and Networks, 2011. 1–9

16 Chang B, Li L, Zhao G, et al. Age of information for actuation update in real-time wireless control systems. In: Proceedings of IEEE Conference on Computer Communications Workshops (INFOCOM WKSHPS), 2020

17 Coffman E G, Liu Z, Weber R R. Optimal robot scheduling for Web search engines. J Sched, 1998, 1: 15–29

18 Cho J, Garcia-Molina H. Synchronizing a database to improve freshness. In: Proceedings of the 2000 ACM SIGMOD International Conference on Management of Data, 2000. 117–128

19 Kaul S, Yates R, Gruteser M. Real-time status: how often should one update? In: Proceedings of IEEE INFOCOM, 2011. 2731–2735

20 Kam C, Kompella S, Ephremides A. Age of information under random updates. In: Proceedings of IEEE International Symposium on Information Theory, 2013. 66–70

21 Kaul S, Yates R, Gruteser M. Status updates through queues. In: Proceedings of the 46th Annual Conference on Information Sciences and Systems (CISS), 2012. 1–6

22 Kaul S, Yates R, Gruteser M. Real-time status: how often should one update? In: Proceedings of IEEE INFOCOM, 2012. 2731–2735

23 Sun Y, Biyikoglu E, Yates R, et al. Update or wait: how to keep your data fresh. IEEE Trans Inform Theory, 2017, 63: 7492–7508

24 Bacinoglu B T, Sun Y, Uysal E, et al. Optimal status updating with a finite-battery energy harvesting source. J Commun Netw, 2019, 21: 280–294

25 Zhong J, Yates R, Soljanin E. Timely lossless source coding for randomly arriving symbols. In: Proceedings of IEEE Information Theory Workshop (ITW), 2018. 1–5

26 Yates R, Ciblat P, Yener A, et al. Age-optimal constrained cache updating. In: Proceedings of IEEE International Symposium on Information Theory (ISIT), 2017. 141–145

27 Ornee T, Sun Y. Sampling for remote estimation through queues: age of information and beyond. In: Proceedings of International Symposium on Modeling and Optimization in Mobile, Ad Hoc, and Wireless Networks (WiOPT), 2019

28 Yang H, Arafa A, Quek T, et al. Age-based scheduling policy for federated learning in mobile edge networks. In: Proceedings of IEEE International Conference on Acoustics, Speech and Signal Processing (ICASSP), 2020

29 Zheng X, Zhou S, Niu Z. Context-aware information lapse for timely status updates in remote control systems. 2019. ArXiv: 1908.04446

30 Ayan O, Vilgelm M, Klugel M, et al. Age-of-information vs. value-of-information scheduling for cellular networked control

systems. In: Proceedings of International Conference on Cyber-Physical Systems, 2019. 109–117

31 Champati J, Mamduhi M, Johansson K, et al. Performance characterization using aoi in a single-loop networked control system. In: Proceedings of IEEE Conference on Computer Communications Workshops (INFOCOM WKSHPS), 2019

32 Ayan O, Vilgelm M, Kellerer W. Optimal scheduling for discounted age penalty minimization in multi-loop networked control. In: Proceedings of the 17th Annual Consumer Communications & Networking Conference (CCNC), 2020

33 Zhang J, Wang C. On the rate-cost of gaussian linear control systems with random communication delays. In: Proceedings of IEEE International Symposium on Information Theory (ISIT), 2018. 2441–2445

34 Yates R D, Kaul S K. The age of information: real-time status updating by multiple sources. IEEE Trans Inform Theor, 2019, 65: 1807–1827

35 Kam C, Molnar J, Kompella S. Age of information for queues in tandem. In: Proceedings of IEEE Military Communications Conference (MILCOM), 2018. 462–467

36 Demirel B, Gupta V, Quevedo D E, et al. On the trade-off between communication and control cost in event-triggered dead-beat control. IEEE Trans Automat Contr, 2017, 62: 2973–2980

37 Klančar G, Škrjanc I. Tracking-error model-based predictive control for mobile robots in real time. Robotics Autonom Syst, 2007, 55: 460–469

38 Shortle J, Thompson J, Gross D, et al. Fundamentals of Queueing Theory. 5th ed. Piscataway: Wiley Press, 2018